JOURNAL OF APPLIED CRYSTALLOGRAPHY

Volume 49 (2016)

Supporting information for article:

Taking a look at the calibration of a CCD detector with a fiber-optic taper

R. W. Alkire, F. J. Rotella, N. E. C. Duke, Zbyszek Otwinowski and Dominika Borek

S1. Procedure for growing lysozyme crystals for beamline calibrations

Lysozyme crystals with low mosaic spread were grown using the following serial dilution, micro-seeding procedure.

Preparation of stock solutions

1. 30% NaCl (w/v) was prepared by dissolving 300.0 grams of sodium chloride in a total volume of 1000 mL of purified water.
2. 1.00 M solutions were prepared of both glacial acetic acid and sodium acetate (NaOAc). Combining these allowed for the preparation of 1.00 M NaOAc, pH 4.75.

Preparation of micro seeds

3. Using a multi-cavity glass depression slide, a large, single lysozyme crystal, was washed twice with 500 μL aliquots of "crystal stabilizer" solution (0.100 M NaOAc, pH 4.75; 24% (w/v) NaCl).
4. The seed crystal was then placed in a third aliquot of 500 μL stabilizer solution, and crushed thoroughly with a small glass rod.
5. The resulting solution was transferred to a 1.5 mL microfuge tube, touched briefly (2-5 seconds) to a low-frequency vortex shaker, then spun for 5-10 seconds at 500 rcf in a desktop microfuge.
6. The resultant supernatant was labelled 1/1× seed stock; serial dilutions were created at 1/10× through 1/10,000×, using stabilizer solution as diluent.

Preparation of protein solution

7. Recently ordered hen egg-white lysozyme of high enzymatic activity (Sigma Aldrich L6876 [crystallized three times, dialyzed, lyophilized powder; ≥40,000 units/mg protein], Sigma-Aldrich, St. Louis, MO, USA) was dissolved in 0.100 M NaOAc solution, pH 4.75 at a concentration of ~100 mg/mL, and dialyzed overnight at 4 °C, against 0.100 M NaOAc, pH 4.75. *Sigma Aldrich #62970 [dialyzed, lyophilized, powder, ~100,000 units/mg] has also been used.*
8. The following morning, the protein solution was spun at 3220 rcf (4 °C) for 30 minutes, filtered through a 0.2 μm low protein-binding syringe-tip filter, brought to a final concentration of 55 mg/mL, and the solution left to incubate at 20 °C for 1 hour.

Crystallization and seeding

9. A multiple-well (Linbro 24-well) plate was set up with 1000 μL reservoirs containing 0.100 M NaOAc, 25% (v/v) ethylene glycol and varying amounts of NaCl; row A contained 4% (w/v), row B 5% (w/v), row C 6% (w/v), and row D 7% (w/v) NaCl.
10. Reservoir solutions were made up in bulk, using 15 mL tubes, then dispensed at 1000 μL per reservoir; this approach allowed for thorough shaking/mixing of the reservoir solution, and

helped maintain consistency between various reservoirs within a row, and from one multi-well plate to another.

11. Protein solution was mixed with reservoir solution at a 1:1 ratio.
12. For 6 drops each at 20 μL, ~150 μL of solution was made up, mixed thoroughly via pipette, then aliquots dispensed at ~20 μL per reservoir.
13. Making up and mixing the bulk quantity of 1:1 protein:reservoir solution helped create greater consistency between drops, across a row.
14. Each of the 6 drops was then spiked with 1 μL of a given seed-stock solution: column 1: stabilizer solution (blank), column 2: 1/1× seed stock, column 3: 1/10× seed stock, column 4: 1/100× seed stock, column 5: 1/1,000× seed stock, column 6: 1/10,000× seed stock.
15. Each seeded drop was carefully "pumped" once or twice with the seeding pipette, to help distribute the seed-stock solution, then the entire drop carefully flipped to form "hanging drop", and sealed over its reservoir.
16. The completed box was labelled and set aside in a vibration-free area, at room temperature (20 ^{o}C), and not disturbed for at least 72 hours.

Observation, analysis, and tips

17. Crystals appeared in less than 24 hours, and continued to grow slowly over 2-3 weeks.
18. Number of crystals and final crystal size varied according to number of seeds available in drop; use of the serial dilution method allowed for finer control of growing conditions and number of resulting crystals.
19. Additional boxes were set, using 26-30% ethylene glycol, with all other conditions as above; crystal growth was slower at higher concentrations of ethylene glycol.
20. All crystals were frozen directly in liquid nitrogen, with no further cryoprotection.
21. Box-like crystals, with nucleation initiated at the surface of the hanging drop and further growth occurring as a projection into the mother liquor, were often observed to have the lowest mosaic spread after freezing. However, all frozen crystals varied in mosaicity, and no visual discrimination could be achieved in advance, using a polarized microscope.
22. The particular crystal used in this study was grown from 0.100 M NaOAc (pH 4.75), 4% (w/v) NaCl, and 27% (v/v) ethylene glycol.

The authors would like to thank Gwyndaf Evans, Youngchang Kim and Changsoo Chang for discussions and valuable advice in the preparation of this procedure.

Figure S1 (a) Photograph showing the small machined face of the fiber-optic taper protruding from the mounting hardware prior to bonding onto a CCD chip. (b) A close-up view of the bundled fibers arranged in a visible hexagonal pattern.

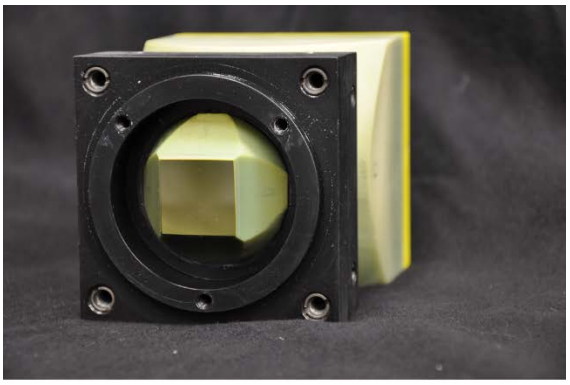

(*a*)

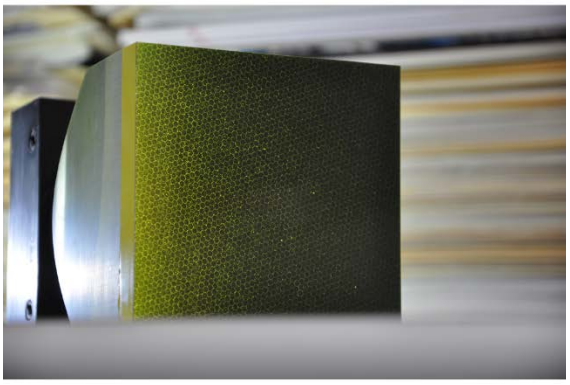

(*b*)

Figure S2 Image of the two reflection locations in the module center and corner used for determining detector linearity. The detector response was found to be linear over a range of 1:330, even when the measured reflections were near the extremes of fiber bending in the taper.

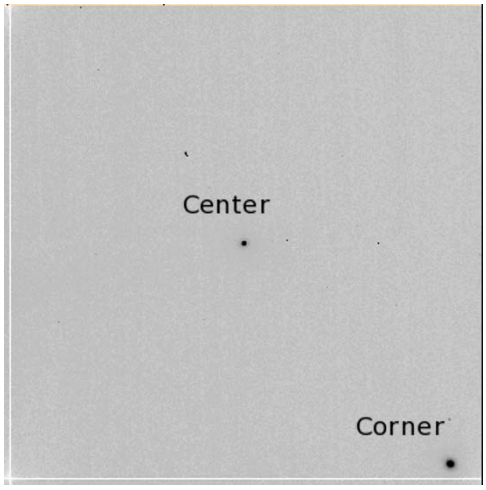

Figure S3 Experimental setup used to illustrate the smoothing features present in a flood-field measurement. Two stainless steel rulers are positioned vertically at different distances away from the edges of a fiber-optic taper. A 100 second exposure using a copper fluorescence source was recorded (as shown). Light (low intensity) areas on the image show the absorption by the two rulers, as they are sufficiently thick to absorb all copper fluorescence radiation. Trends for smoothing as a function of fiber bend are similar along the comparable edges of both rulers. Because the ruler on the right, closest to the detector center, is a few millimeters farther from the edge of the fiber-optic taper than the one on the left, the intensity path leading to the ruler's edge is longer, making the transition to the edge easier to follow visually. For this reason only, data from the ruler on the right were chosen for presentation in this study. Distance from the right ruler's edge to the detector centerline is approximately 4.5 mm.

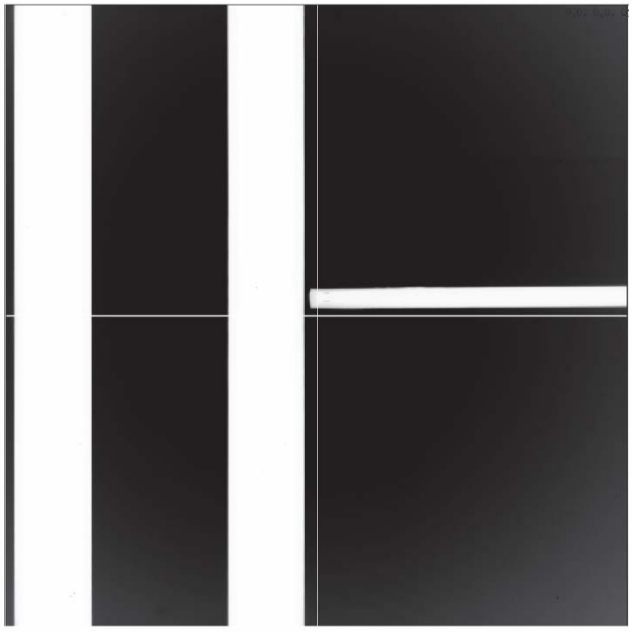

Figure S4 Polynomial fit of integrated intensity values derived from Figure 5 along a line from the center of the module to the corner. Fit parameters are shown in the figure inset. Using these fit parameters, corrections to intensity losses were computed, generating new Si(311) intensities shown in Figure 10.